AGU PUBLICATIONS

Geophysical Research Letters

RESEARCH LETTER
10.1002/2016GL070274

Key Points:
- Prolonged El Nino conditions during 2014-2015 drove record-high SST and sea surface height in the northeastern tropical Pacific
- Record-high SST, deeper than normal thermocline, and low surface salinity contributed to Patricia's intensification
- SST anomalies in the northeastern Pacific were driven mainly by anomalously deep thermocline and reduced vertical turbulent cooling

Supporting Information:
- Supporting Information S1

Correspondence to:
G. R. Foltz,
gregory.foltz@noaa.gov

Citation:
Foltz, G. R. and K. Balaguru (2016), Prolonged El Niño conditions in 2014–2015 and the rapid intensification of Hurricane Patricia in the eastern Pacific, *Geophys. Res. Lett.*, *43*, 10,347–10,355, doi:10.1002/2016GL070274.

Received 1 JUL 2016
Accepted 22 AUG 2016
Accepted article online 25 AUG 2016
Published online 7 OCT 2016

Prolonged El Niño conditions in 2014–2015 and the rapid intensification of Hurricane Patricia in the eastern Pacific

Gregory R. Foltz[1] and Karthik Balaguru[2]

[1]NOAA/Atlantic Oceanographic and Meteorological Laboratory, Miami, Florida, USA, [2]Marine Sciences Laboratory, Pacific Northwest National Laboratory, Seattle, Washington, USA

Abstract Hurricane Patricia was the most intense tropical cyclone on record in the eastern North Pacific or Atlantic, reaching a peak intensity of 95 m s^{-1} only 30 h after attaining hurricane status (33 m s^{-1}). Here it is shown that exceptionally warm sea surface temperatures (SSTs), a deeper than normal thermocline, and strong near-surface salinity stratification all aided Patricia's rapid intensification, combining to increase its Potential Intensity by 1–14 m s^{-1}. Anomalous surface warming and thermocline deepening along Patricia's track were driven by prolonged El Niño conditions during 2014–2015 and punctuated by the buildup to the extreme El Niño of 2015–2016. In the region where Patricia intensified, SST was 1.5° C higher and sea surface height was 10 cm higher compared to conditions during the last extreme El Niño in 1997, emphasizing the extraordinary nature of the 2015 anomalies.

1. Introduction

The 2015 Northeast Pacific hurricane season was the second most active on record and produced an unprecedented 11 major hurricanes (maximum sustained wind of at least 50 m s^{-1}). Patricia was unique among these storms because of its exceptionally high peak intensity and ultimate landfall as a major hurricane along the southwestern coast of Mexico. After forming on 20 October, Patricia underwent a period of very rapid intensification during 22–23 October, increasing from 39 m s^{-1} to 93 m s^{-1} in a 24 h period. Its peak intensity of 95 m s^{-1} (category 5), with a central pressure of 873 hPa, makes it the strongest hurricane on record in the eastern North Pacific and North Atlantic and the second strongest worldwide. Patricia weakened to 67 m s^{-1} (category 4) as it reached Mexico's coast but was still the most intense hurricane to make landfall in Mexico [*Kimberlain et al.*, 2016].

In October 2015, the region in the northeastern tropical Pacific where Patricia intensified experienced the highest sea surface temperatures on record (Figure 1a) [*Kimberlain et al.*, 2016]. Record or near-record sea surface temperatures (SSTs) were also present in the eastern equatorial Pacific, associated with a developing "super" El Niño [*Levine and McPhaden*, 2016], and in the Northeast Pacific due to a large area of strong and persistent sea level pressure anomalies [*Bond et al.*, 2015]. Higher SSTs translate to a higher maximum Potential Intensity for a hurricane [*Emanuel*, 1999], suggesting that the anomalous warmth during October 2015 may have fueled Patricia's extraordinary strengthening. Recent studies have also found a strong relationship between interannual variability of upper ocean heat content and eastern Pacific hurricane activity [*Balaguru et al.*, 2013; *Jin et al.*, 2014], opening up the possibility that subsurface temperature anomalies also may have played a role. Here we examine the upper ocean conditions in the northeastern tropical Pacific and their contribution to Patricia's rapid intensification.

2. Data and Methods

Patricia's 1 min sustained maximum wind speed and location every 6 h were obtained from the National Hurricane Center [*Landsea and Franklin*, 2013]. A monthly blended satellite in situ SST product on a 1° × 1° grid from 1982 to 2015 [*Reynolds et al.*, 2002], daily sea surface height (SSH) anomalies with respect to a 20 year mean, on a $\frac{1}{4}$° grid for 1993–2015 [*Le Traon et al.*, 1998], and monthly surface salinity on a $\frac{1}{4}$° grid from the Soil Moisture and Ocean Salinity [*Kerr et al.*, 2001] satellite sensor are used to examine the large-scale conditions in the eastern Pacific during 2014–2015. Wind velocity at a height of 10 m is available from the ERA-interim reanalysis [*Dee et al.*, 2011] on a daily 0.75° × 0.75° grid from 1982 to 2015. These data are used to examine the

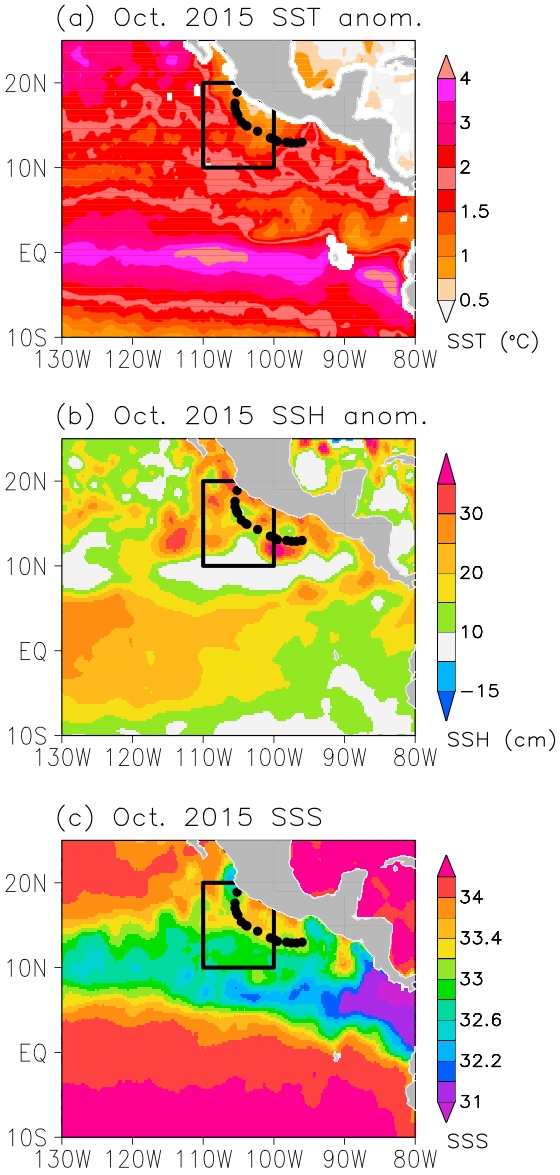

Figure 1. October 2015 anomalies (with respect to 1993–2014 monthly mean climatologies) of (a) satellite in situ SST and (b) satellite SSH. (c) October 2015 sea surface salinity. Black circles in Figures 1a–1c show 6-hourly locations of Patricia, and black boxes indicate region used for area averages shown in Figures 4 and 5.

conditions during 2014–2015 and to calculate Ekman pumping velocity, $w_e = -\nabla \times \left(\frac{\tau}{\rho f}\right)$, where τ is surface wind stress, calculated using a wind speed-dependent drag coefficient [*Donelan et al.*, 2004], ρ is the density of air, and f is the Coriolis parameter.

ERA-interim air temperature, relative humidity, and sea level pressure were used to calculate the atmospheric contribution to Patricia's Dynamic Potential Intensity (DPI) [*Balaguru et al.*, 2015], a variant of Potential Intensity that accounts for cyclone-induced SST cooling. The ocean cooling induced by Patricia for different ocean conditions was estimated using monthly temperature and salinity from National Centers for Environmental Prediction's Global Ocean Data Assimilation System (GODAS) [*Behringer and Xue*, 2004], available from 1980 to 2015 on a $\frac{1}{3}°$ latitude × 1° longitude grid. The methods for calculating DPI and ocean cooling are described later in this section.

To diagnose the causes of large-scale SST variability in the northeastern tropical Pacific during 2014–2015, we perform a mixed layer temperature budget analysis using monthly 1° × 1° surface heat fluxes from the TropFlux product [*Kumar et al.*, 2012], together with the Relynolds et al. SST and monthly Ocean Surface Current Analysis-Realtime (OSCAR) horizontal velocity, averaged from the surface to a depth of 30 m and available during 1993–2015 on a 1° × 1° grid [*Bonjean and Lagerloef*, 2002]. The temperature budget can be expressed as

$$\frac{\partial T_s}{\partial t} = \frac{Q_0}{\rho c h} - \mathbf{v} \cdot \nabla T_s + w_{\text{mix}}. \qquad (1)$$

In (1), T_s is SST, Q_0 is the net surface heat flux, ρ is the density of seawater, c is the capacity, h is mixed layer depth, $\mathbf{v}$ is horizontal velocity averaged in the mixed layer, and w_{mix} represents changes in SST due to the vertical turbulent exchange of heat across the base of the mixed layer. Monthly Reynolds et al. SST is used for T_s, and its horizontal gradient over a distance of 1° is used with monthly OSCAR currents to calculate horizontal temperature advection. The Q_0 term is calculated from TropFlux monthly surface heat fluxes and adjusted for the penetration of solar radiation through the mixed layer: $S_{\text{pen}} = S_0 e^{-h/15}$, where S_0 is the downward surface solar radiation. Mixed layer depth is calculated from monthly GODAS temperature and salinity using the criterion of a 0.07 kg m^{-3} density increase from a depth of 5 m. Because w_{mix} is difficult to calculate directly, we estimate it as the difference between the rate of change of SST (first term in (1)) and the sum of the net surface heat flux and temperature advection (first two terms on the righthand side of (1)).

To assess the impact of upper ocean conditions on Patricia's development, we consider the along-track SST cooling and DPI, in addition to the larger-scale analyses described earlier in this section. To estimate the SST

cooling induced by Patricia, we first follow *Balaguru et al.* [2015] and estimate the maximum depth to which mixing occurred during Patricia's passage through a given 6-hourly location:

$$L = h + \left(\frac{2\rho_o {u_*}^3 t}{\kappa g \alpha} \right)^{\frac{1}{3}} \tag{2}$$

where h is the initial mixed layer depth, ρ_o is the seawater density, u_* is the friction velocity, t is the time period of mixing, κ is the von Kármán constant, g is the acceleration due to gravity, and α is the rate of increase of potential density with depth from the base of the mixed layer to 50 m below the mixed layer. This formula explicitly accounts for the influence of temperature and salinity stratification on the mixing length. We use October 2015 temperature and salinity from GODAS to calculate h, averaged in a 2° × 2° box and centered on each 6-hourly location. The u_* term is computed from the observed peak storm wind speed, with a drag coefficient that is accurate for high winds [*Donelan et al.*, 2004]. The parameter $t = R/U$ is calculated as the time for the storm moving at its observed translation speed to cross a distance of R =8 km, the approximate average radius of maximum winds during Patricia's intensification stage.

With the mixing length from (2), we calculate the vertically averaged temperature from the surface to L at each 6-hourly location:

$$T_{dy} = \frac{1}{L} \int_0^L T(z) \mathrm{d}z. \tag{3}$$

T_{dy} therefore represents an estimate of the SST that is experienced by Patricia's core. The SST cold wake is calculated as T_{dy} minus the 2° × 2° area-average of GODAS October 2015 SST, centered on each storm location. The DPI is calculated as

$$\mathrm{DPI}^2 = \frac{T_{dy} - T_o}{T_o} \frac{C_K}{C_D} \left(k_{T_{dy}} - k \right) \tag{4}$$

where DPI represents the maximum wind speed of Patricia, T_o is the outflow temperature, C_D is the coefficient of drag, C_K is the coefficient of enthalpy exchange, $k_{T_{dy}}$ is the enthalpy of air in contact with the sea surface, and k is the specific enthalpy of air near the surface in the storm environment. ERA-interim air temperature and relative humidity for the month of October 2015 are used to calculate T_o, $k_{T_{dy}}$, and k. Standard bulk formulas for latent and sensible heat fluxes are used to calculate enthalpy, and C_K/C_D is set to the default value of 0.9 [*Bister and Emanuel*, 2002]. In order to examine the influence of the ocean state on the cold wake and DPI, we perform three additional analyses consisting of the same calculations except we use either (1) climatological October temperature, salinity, air temperature, and humidity, (2) October 1997 conditions, and (3) October 2015 conditions except salinity is set to zero at all depths before calculating L. The first two analyses are used to examine the extent to which anomalous conditions in 2015, relative to climatology and 1997, contributed to Patricia's development. The year 1997 was chosen because the strong El Niño conditions in the equatorial Pacific in that year were very similar to those in 2015. The last analysis is used to examine the extent to which salinity may have contributed to Patricia's intensification.

3. Results

In October 2015, there were above normal SSTs in most of the eastern tropical Pacific. The positive anomalies peaked on the equator in association with the developing El Niño, and there was a secondary peak in the northern subtropics due to the southeastward movement of the North Pacific "warm blob" [*Bond et al.*, 2015] (Figure 1a). The sea surface was higher than normal between 10°N and 18°N and east of 120°W (Figure 1b). In general, these anomalies are consistent with El Niño-forced equatorial Kelvin wave reflection at the eastern boundary and subsequent westward Rossby wave radiation [*Enfield and Allen*, 1980; *Fu and Qiu*, 2002], combined with anomalous downwelling-favorable wind stress curl [*Fu and Qiu*, 2002; *Abe et al.*, 2014]. There is also evidence of anticyclonic eddies centered near 12°N, possibly driven by enhanced easterly winds through gaps in the central American mountains [*Willett et al.*, 2006]. Positive SSH anomalies translated to an anomalously deep thermocline and thick mixed layer in the northeastern tropical Pacific (Figures S1–S3 in the supporting information). As Patricia turned northward and approached Mexico, it encountered surface water that was ~ 0.3 practical salinity unit fresher (Figure 1c). This fresher water was present before Patricia's arrival and is

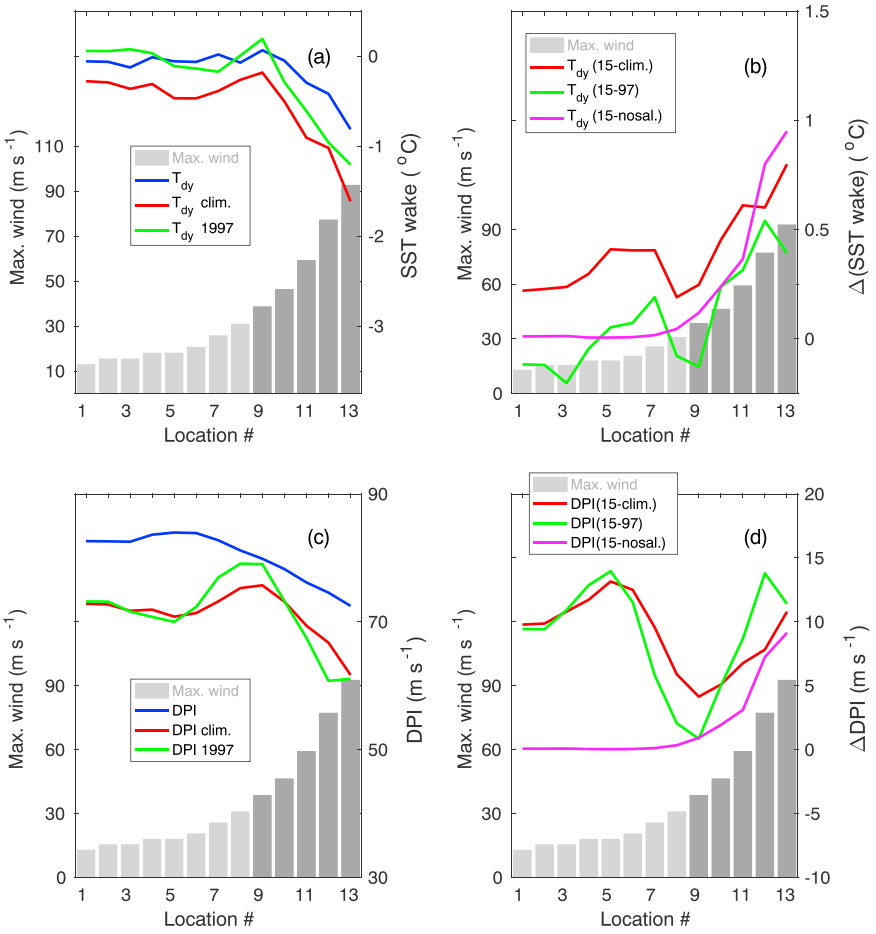

Figure 2. (a) Maximum wind speed of Patricia at 6-hourly locations from 6Z 20 October to 6Z 23 October (gray bars, with dark gray indicating an intensification rate of more than 15 m s^{-1} per 12 h), SST cold wake calculated from T_{dy} with monthly GODAS temperature and salinity from October 2015 (blue), from T_{dy} with climatological temperature and salinity (red), and T_{dy} with temperature and salinity from October 1997 (green). (b) Same as Figure 2a except difference between the cold wake calculated using 2015 conditions and climatological conditions (red), between cold wake using 2015 and 1997 conditions (green), and between cold wake using 2015 conditions and 2015 conditions with no salinity (purple). (c and d) Same as Figures 2a and 2b except for DPI.

likely due to outflow from the Rio Grande de Santiago and Balsas Rivers, which enter the ocean at 21°N and 18°N, respectively (Figure S4).

The anomalously deep thermocline along Patricia's track acted to reduce SST cooling by about 0.2–0.8°C relative to the cooling that would have occurred under climatological conditions (Figures 2a and 2b). There is a reduction in the cold wake magnitude of up to 0.5°C even relative to 1997, when conditions in the equatorial Pacific were very similar to 2015, emphasizing the unusual nature of the upper ocean temperature anomalies in the northeastern tropical Pacific in 2015. As Patricia underwent rapid intensification (rapid intensification here is defined as an increase of at least 15 m s^{-1} in a 12 h period), it traveled over low-salinity waters with strong stratification (Figures 1c and S5), which tended to suppress vertical mixing and SST cooling (Figure 2b). Though the mean salinity structure was important, we found that salinity anomalies did not contribute substantially to Patricia's cold wake. Good agreement between the estimated and observed cold wakes (Figure S6) suggests that our cold wake model is reasonable and that the comparison based on different background conditions is meaningful.

Consistent with the cold wake analysis, the ocean state in October 2015 was more conducive to intensification compared to the climatological state or conditions in 1997 (Figures 2c and 2d). Anomalous upper ocean conditions (either relative to 1997 or climatology) enhanced DPI by 1–14 m s^{-1} during the period when Patricia's strength increased from 59 to 93 m s^{-1} (low-end category 4 to strongest hurricane on record in the

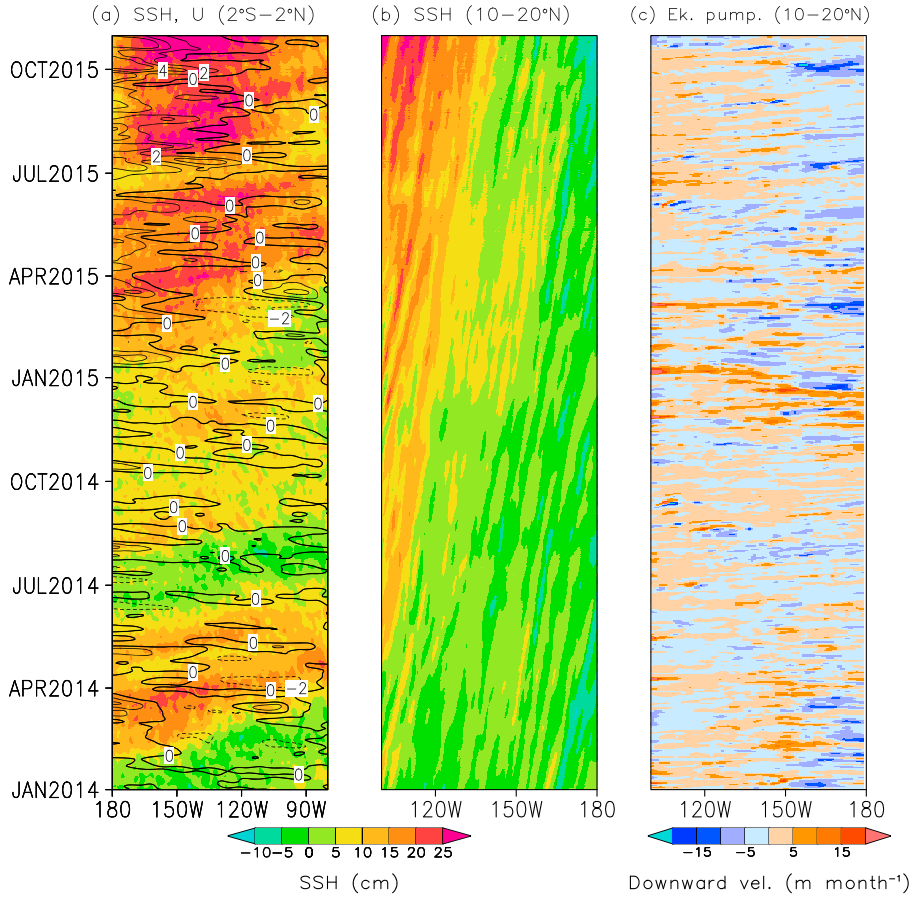

Figure 3. (a) Anomalies of SSH (shaded) and zonal 10 m wind (contours) averaged between 2°S and 2°N. (b) Same as Figure 3a except wind anomalies are not shown and SSH is averaged in the 10°N–20°N band centered on Patricia (shown in Figure 1). (c) Same as Figure 3b except Ekman pumping velocity (positive downward). The *x* axis (longitude) in Figures 3b and 3c for has been reversed to show the westward propagating Rossby wave signal resulting from reflection at the eastern boundary.

Northeast Pacific or Atlantic). Atmospheric conditions did not contribute substantially to the DPI (Figure S7). Results are similar when a one-dimensional numerical mixed layer model is used to calculate Patricia's SST wake and DPI, except that the cold wake estimated using 1997 background conditions is weaker and the suppression of cooling due to salinity is weaker (Text S1 and Figure S8). Note that the DPI decreases along Patricia's track as its intensity increases rapidly (Figure 2c). This is likely due to a cold bias in GODAS SST, which generates a low bias in DPI that is largest toward the end of Patricia's track (Figure S9). It is also likely that the cold SST bias results in upper ocean stratification that is too weak and a cold SST wake that is too strong, further depressing DPI. It is therefore probable that the upper ocean conditions were even more favorable for intensification than indicated in Figure 2.

The cold wake and DPI analyses show that Patricia benefited from strong anomalous warming in the upper ocean prior to October 2015. The causes of the subsurface warming can be traced to conditions in the equatorial Pacific beginning in early 2014. Between January and April, westerly wind anomalies in the central and western equatorial Pacific forced downwelling equatorial Kelvin waves (Figures 3a and 3b). The Kelvin waves propagated eastward, reflected into coastal Kelvin waves and westward propagating Rossby waves at the eastern boundary, and consequently increased SSH in the eastern basin between 10 and 20°N, where Patricia strengthened (Figures 3a and 3b) [*Menkes et al.*, 2014; *McPhaden*, 2015]. Subsequent equatorial easterly wind anomalies during June–July temporarily halted the developing El Niño and the anomalous increase in SSH between 10 and 20°N (Figures 3a and 3b) [*Hu and Fedorov*, 2016; *Levine and McPhaden*, 2016]. Westerly wind anomalies resumed in early 2015, reviving El Niño conditions and contributing to a ~10 cm anomalous increase of SSH in the eastern Pacific between 10 and 20°N (Figures 3a and 3b) [*Levine and McPhaden*, 2016].

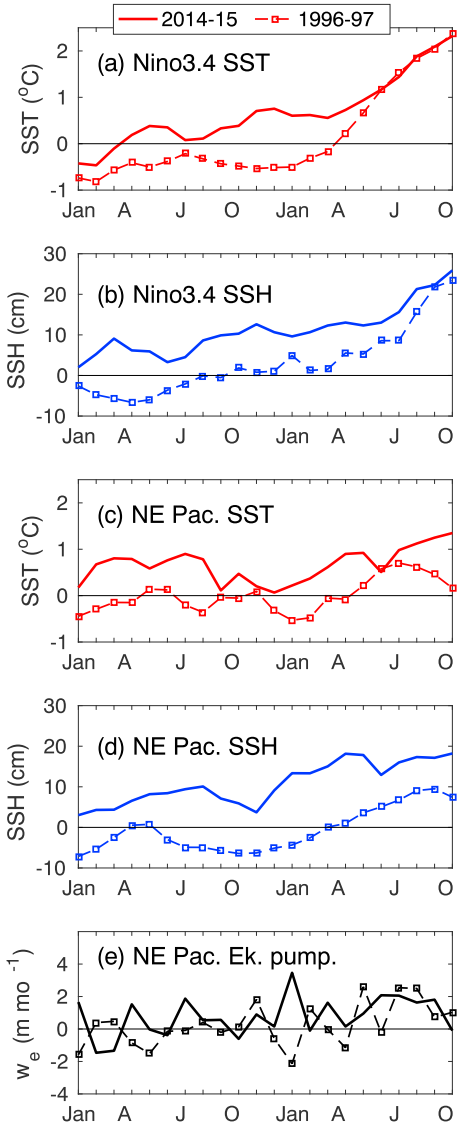

Figure 4. Monthly anomalies during January 2014–October 2015 (solid) and January 1996–October 1997 (dashed with squares): Niño3.4 (a) SST and (b) SSH; (c) SST, (d) SSH, and (e) Ekman pumping (positive downward) averaged in the Patricia region (shown in Figure 1).

As the El Niño strengthened during July–October 2015, anomalous Ekman pumping between 10 and 20°N further increased SSH (Figure 3c). The tendency for reflected planetary waves and local Ekman pumping anomalies in the northeastern tropical Pacific to increase SSH during the 2014–2015 El Niño is consistent with results for a composite El Niño [*Enfield and Allen*, 1980; *Fu and Qiu*, 2002; *Abe et al.*, 2014]. However, as will be discussed in the remainder of this section, the anomalies in 2015 were considerably larger, even in comparison to 1997, arguably the strongest El Niño on record.

The development of the strong El Niño in 2015 was preceded by 9 months of positive Niño3.4 SST anomalies (averaged 5°S–5°N, 120°W–170°W) going back to April 2014 (Figure 4a). The combined duration and peak strength of the Niño3.4 SST anomalies in 2014–2015 is unprecedented going back to the start of the satellite era in 1982. In contrast, SST anomalies were negative during all of 1996 and turned positive only in April 1997 leading up to the 1997–1998 El Niño. These differences were present despite almost identical conditions in the equatorial Pacific during the months of June–October in 1997 and 2015 (Figure 4a). Equatorial Pacific SSH anomalies and northeastern tropical Pacific SST anomalies were positive during all of 2014 and 2015, consistent with the prolonged El Niño (Figures 4b and 4c). The equatorial warming and eastward Kelvin wave propagation led to an anomalous increase in SSH in the northeastern tropical Pacific of 15 cm from January 2014 to October 2015, similar to the anomalous increase during the same period in 1996-1997 (Figure 4d). However, SSH in October 2015 was 10 cm higher than in October 1997 because of preconditioning from the unusually persistent El Niño conditions extending back to early 2014. Forcing of the SSH anomalies in the northeastern tropical Pacific during 2014–2015 likely came from the combination of reflected coastal Kelvin and Rossby waves and local Ekman pumping (Figures 3 and 4e).

The causes of anomalous surface warming in the northeastern tropical Pacific during a typical El Niño are not well known [*Karnauskas and Busalacchi*, 2009; *Alexander et al.*, 2012], and the presence of record warmth in the subtropical northeastern Pacific during 2015 adds to the intrigue regarding the anomalous warming prior to Patricia. During a typical El Niño, atmospheric convection and cloudiness in the northeastern tropical Pacific shift southward toward the strongest SST anomalies on the equator [*Karnauskas and Busalacchi*, 2009]. However, during 2014–2015 there was weaker heating from surface solar radiation in the northeastern tropical Pacific compared to the same period in 1996–1997 due to enhanced cloudiness (Figure 5a). There was also more cooling from the surface latent heat flux in 2014–2015 compared to 1996–1997, consistent with higher rates of evaporation from warmer SST in 2014–2015. Combined, the absorbed solar radiation and latent heat flux tended to cool SST more strongly in 2014–2015 and therefore cannot explain the anomalous warmth relative to 1996–1997. Differences in longwave radiation and sensible heat flux were generally much weaker in comparison. When the anomalously thick mixed layer during 2014–2015 is taken into account, cooling from the net surface heat flux was even stronger relative to 1996–1997 (Figure 5a).

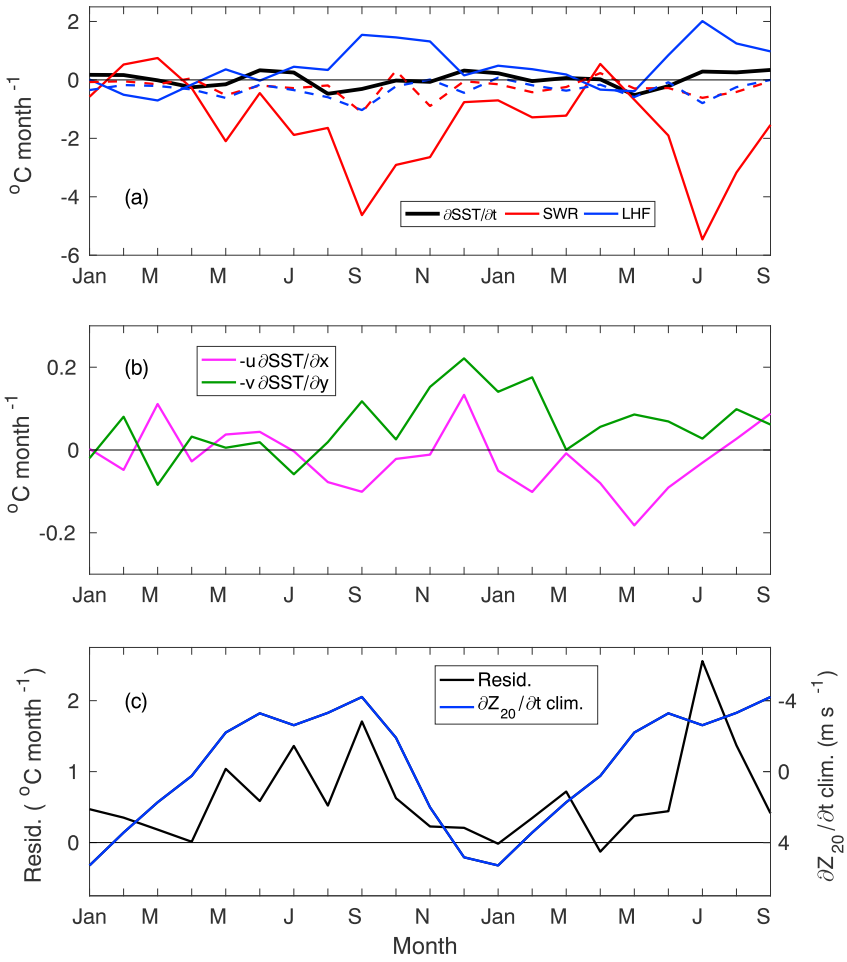

Figure 5. January 2014–September 2015 monthly anomalies averaged in the Patricia region (shown in Figure 1). (a) Rate of change of SST (black), surface shortwave radiation corrected for penetration through the based of the mixed layer, calculated with climatological mixed layer depth (MLD) (dashed red) and full mixed layer depth (solid red), and latent heat flux (dashed blue: climatological MLD, solid blue: full MLD). Positive indicates tendency to increase SST. (b) Same as Figure 5a except zonal (pink) and meridional (green) mixed layer temperature advection. (c) Same as Figure 5a except temperature budget residual (black: $\partial SST/\partial t$ minus sum of surface heat fluxes and advection) and climatological rate of change of the 20°C isotherm depth (blue).

Another candidate for the cause of the anomalous warmth in the northeastern tropical Pacific is the record warmth in the North Pacific [*Bond et al.*, 2015]. There is evidence that mean southward near-surface currents transported anomalous warmth into the northeastern tropical Pacific during August 2014–September 2015 (Figure 5b). However, the net increase in SST due to meridional advection is 1.3°C during this period relative to the same period in 1996–1997, compared to −9.3°C from the surface heat flux. The record warmth in the northeastern tropical Pacific during 2015 therefore cannot be explained by the combination of the surface heat flux and horizontal advection. Instead, anomalous Ekman downwelling, and associated deepening of the thermocline and reduction in vertical turbulent cooling, appear to be the dominant causes. There is evidence that the anomalous warming from vertical advection and mixing (estimated from the difference between the rate of change of SST and the sum of horizontal advection and the surface heat flux) is strongest during the months when the climatological thermocline is shoaling and SST is most likely to be influenced by thermocline depth anomalies (Figure 5c). Further support for the importance of vertical processes comes from the positive correlations between monthly anomalies in SST and SSH in the northeastern tropical Pacific during January 2014–September 2015 (0.53, significant at the 5% level) and August 2014–September 2015 (0.75, significant at the 5% level), when southward advection of the North Pacific warm blob appears to have been strongest (Figures 4c and 4d).

4. Summary and Discussion

In the unusually active eastern Pacific hurricane season of 2015, Patricia stands out for its very rapid intensification and record-breaking peak intensity. Here we examined the upper ocean conditions in the northeastern tropical Pacific leading up to Patricia, focusing on the role of the upper ocean in Patricia's intensification and the ultimate causes of strong upper ocean temperature anomalies. We found that anomalous warmth and a deeper than normal thermocline in October 2015 acted to reduce Patricia's cold wake by 0.2–0.8°C and increase its Dynamic Potential Intensity by 1–14 m s^{-1} during the period of rapid intensification. The mean salinity structure, consisting of a thin, fresh surface layer, and strong stratification beneath, tended to limit cooling from turbulent mixing. Combined, the upper ocean temperature anomalies and mean salinity structure made the environment considerably more favorable for intensification.

The main cause of the anomalously deep thermocline and upper ocean warmth in the northeastern tropical Pacific Ocean was traced to conditions in the equatorial Pacific beginning in early 2014. A developing El Niño in early 2014 began to deepen the thermocline anomalously in the northeastern tropical Pacific through planetary wave propagation and local Ekman pumping. Weak to moderate El Niño conditions continued through early 2015, further depressing the thermocline and setting the stage for record anomalous warmth and sea surface height in the northeastern tropical Pacific in October 2015 as the strong 2015–2016 El Niño matured. Our mixed layer temperature budget analysis revealed that neither surface heat fluxes nor horizontal temperature advection can explain the anomalous surface warming that took place in the northeastern tropical Pacific during 2014–2015. Instead, the anomalously deep thermocline and associated reduction in vertical advection and mixing were the main factors.

Patricia's rapid intensification during 22–23 October was very poorly predicted by the National Hurricane Center's official intensity forecast, with low biases of 31–54 m s^{-1} (60–105 kt) at lead times of 12–48 h [*Kimberlain et al.*, 2016]. Though imperfect knowledge of the atmospheric state and internal hurricane dynamics likely played a role, it is also possible that some models' failure to account properly for the strong subsurface temperature anomalies and mean salinity stratification may have contributed to the severe underestimation of Patricia's intensity. Further quantification of the role of salinity in tropical cyclone intensification and the potential for improved intensity forecasts through the inclusion of salinity would be helpful, based on the importance of salinity shown in this study and others [*Balaguru et al.*, 2012; *Domingues et al.*, 2015]. In this study, we focused on the role of the ocean in Patricia's intensification. Further studies examining the impact of the atmosphere are needed for a more complete understanding of Patricia's extraordinary strength.

Acknowledgments

G.F. was supported by base funds to NOAA's Atlantic Oceanographic and Meteorological Laboratory. K.B. was supported by the U.S. Department of Energy (DOE) Office of Science's Biological and Environmental Research Regional and Global Climate Modeling prgram. Pacific Northwest National Laboratory (PNNL) is operated for DOE by Battelle Memorial Institute under contract DE-AC05-76RL01830. We thank Ricardo Domingues and two anonymous reviewers for their suggestions that improved the manuscript. All data and models used in this study are freely available, as described in the references given in section 2 and the supporting information, or can be obtained from gregory.foltz@noaa.gov upon request.

References

Abe, H., Y. Tanimoto, T. Hasegawa, N. Ebuchi, and K. Hanawa (2014), Oceanic Rossby waves induced by the meridional shift of the ITCZ in association with ENSO events, *J. Oceanogr.*, *70*, 165–174.

Alexander, M. A., H. Seo, S.-P. Xie, and J. D. Scott (2012), ENSO's impact on the gap wind regions of the eastern tropical Pacific Ocean, *J. Clim.*, *25*, 3549–3565.

Balaguru, K., P. Chang, R. Saravanan, L. R. Leung, Z. Xu, M. K. Li, and J.-S. Hsieh (2012), Ocean barrier layers' effect on tropical cyclone intensification, *Proc. Natl. Acad. Sci. U.S.A.*, *109*, 14,343–14,347.

Balaguru, K., L. R. Leung, and J.-H. Yoon (2013), Oceanic control of Northeast Pacific hurricane activity at interannual timescales, *Environ. Res. Lett.*, *8*, 44009, doi:10.1088/1748-9326/8/4/044009.

Balaguru, K., G. R. Foltz, L. R. Leung, E. A. D'Asaro, K. A. Emanuel, H. Liu, and S. E. Zedler (2015), Dynamic Potential Intensity: An improved representation of the ocean's impact on tropical cyclones, *Geophys. Res. Lett.*, *42*, 6739–6746, doi:10.1002/2015GL064822.

Bister, M., and K. A. Emanuel (2002), Low frequency variability of tropical cyclone potential intensity 1. Interannual to interdecadal variability, *J. Geophys. Res.*, *107*(D24), 4801, doi:10.1029/2001JD000776.

Behringer, D. W., and Y. Xue (2004), Evaluation of the Global Ocean Data Assimilation System at NCEP: The Pacific Ocean, paper 2.3 presented at Eighth Symposium on Integrated Observing and Assimilation Systems for Atmosphere, Oceans, and Land Surface, Am. Meteorol. Soc., Seattle, Wash., Preprints. [Available at: http://ams.confex.com/ams/84Annual/techprogram/paper_70720.htm.]

Bond, N. A., M. F. Cronin, H. Freeland, and N. Mantua (2015), Causes and impacts of the 2014 warm anomaly in the NE Pacific, *Geophys. Res. Lett.*, *42*, 3414–3420, doi:10.1002/2015GL063306.

Bonjean, F., and G. S. E. Lagerloef (2002), Diagnostic model and analysis of the surface currents in the tropical Pacific Ocean, *J. Phys. Oceanogr.*, *32*, 2938–2954.

Dee, D. P., et al. (2011), The ERA-Interim reanalysis: Configuration and performance of the data assimilation system, *Q. J. R. Meteorol. Soc.*, *137*, 553–597, doi:10.1002/qj.828.

Domingues, R., et al. (2015), Upper ocean response to Hurricane Gonzalo (2014): Salinity effects revealed by targeted and sustained underwater glider observations, *Geophys. Res. Lett.*, *42*, 7131–7138, doi:10.1002/2015GL065378.

Donelan, M., B. K. Haus, N. Reul, W. J. Plant, M. Stiassnie, H. C. Graber, O. B. Brown, and E. S. Saltzman (2004), On the limiting aerodynamic roughness of the ocean in very strong winds, *Geophys. Res. Lett.*, *31*, L18306, doi:10.1029/2004GL019460.

Emanuel, K. A. (1999), Thermodynamic control of hurricane intensity, *Nature*, *401*, 665–669.

Enfield, D. B., and J. S. Allen (1980), On the structure and dynamics of monthly mean sea level anomalies along the Pacific coast of North and South America, *J. Phys. Oceanogr.*, *10*, 557–588.

Fu, L.-L., and B. Qiu (2002), Low-frequency variability of the North Pacific Ocean: The roles of boundary- and wind-driven baroclinic Rossby waves, *J. Geophys. Res.*, *107*(C12), 3220, doi:10.1029/2001JC001131.

Hu, S., and A. V. Fedorov (2016), Exceptionally strong easterly wind burst stalling El Niño of 2014, *Proc. Natl. Acad. Sci. U.S.A.*, *113*, 2005–2010.

Jin, F.-F., J. Boucharel, and I.-I. lin (2014), Eastern Pacific tropical cyclones intensified by El Niño delivery of subsurface ocean heat, *Nature*, *516*, 82–88.

Karnauskas, K. B., and A. J. Busalacchi (2009), Machanisms for the interannual variability of SST in the East Pacific warm pool, *J. Clim.*, *22*, 1375–1392.

Kerr, Y. H., P. Waldteufel, J. P. Wigneron, J. M. Martinuzzi, J. Font, and M. Berger (2001), Soil moisture retrieval from space: The Soil Moisture and Ocean Salinity (SMOS) mission, *IEEE Trans. Geosci. Remote Sens.*, *39*, 1729–1735.

Kimberlain, T. B., E. S. Blake, and J. P. Cangialosi (2016), Hurricane Patricia, Natl. Hurricane Center Trop. Cyclone Rep. NOAA, Miami, Fla. [Available at: http://www.nhc.noaa.gov/data/tcr/EP202015_Patricia.pdf.]

Kumar, B. P., J. Vialard, M. Lengaigne, V. S. N. Murty, and M. J. McPhaden (2012), TropFlux: Air-sea fluxes for the global tropical oceans—Description and evaluation, *Clim. Dyn.*, *38*, 1521–1543, doi:10.1007/s00382-011-1115-0.

Landsea, C. W., and J. L. Franklin (2013), Atlantic Hurricane database uncertainty and presentation of a new database format, *Mon. Weather Rev.*, *141*, 3576–3592.

Le Traon, P. Y., F. Nadal, and N. Ducet (1998), An improved mapping method of multisatellite altimeter data, *J. Atmos. Oceanic Technol.*, *15*, 522–533.

Levine, A. F. Z., and M. J. McPhaden (2016), How July 2014 easterly wind burst gave the 2015–2016 El Niño a head start, *Geophys. Res. Lett.*, *43*, 6503–6510, doi:10.1002/2016GL069204.

McPhaden, M. J. (2015), Playing hide and seek with El Niño, *Nat. Clim. Change*, *5*, 791–795.

Menkes, C. E., et al. (2014), About the role of westerly wind events in the possible development of an El Niño in 2014, *Geophys. Res. Lett.*, *41*, 6476–6483, doi:10.1002/2014GL061186.

Reynolds, R. W., N. A. Rayner, T. M. Smith, D. C. Stokes, and W. Q. Wang (2002), An improved in situ and satellite SST analysis for climate, *J. Clim.*, *15*, 1609–1625.

Willett, C. S., R. R. Leben, and M. F. Lavín (2006), Eddies and tropical instability waves in the eastern tropical Pacific: A review, *Prog. Oceanogr.*, *69*, 218–238.